archives
of thermodynamics
Vol. **31**(2010), No. 3, 37–53
DOI: 10.2478/v10173-010-0013-x

Investigation of the flow conditions in a high-performance heat exchanger

STANISŁAW ŁOPATA*
PAWEŁ OCŁOŃ

Cracow University of Technology, Division of Power Engineering, al. Jana Pawła II 37, 31-864 Kraków, Poland

Abstract CFD (Computational Fluid Dynamics) computations are carried out in order to investigate the flow distribution and its influence on the heat transfer processes in the high-performance heat exchanger. The subject of this investigation is the classical model of the high-performance heat exchanger with elliptical tubes and rectangular fins. It is possible to find the flow domains where the heat transfer conditions are impaired due to the fully developed turbulent flow. Therefore, the considerable thermal loads occur that may cause the breakdown of the heat exchanger. The emphasis of this investigation is put on the zones and the locations where the tubes are not properly fed with liquid, that result in occurrence of cavitation.

Keywords: Heat exchange; Failure; Computational simulation

Nomenclature

c_{pw}	–	heat capacity of water, W/(m K)
C_μ	–	k-ε turbulence model constant, $C_\mu = 0.09$
d_m	–	mean diameter, m
e_l	–	element's edge length, mm
F_c	–	cross sectional area of fluid domain in collector, m^2
F_{in}	–	cross sectional area of inlet domain, m^2

*Corresponding author. E-mail address: lopata@mech.pk.edu.pl

F_t	–	cross sectional area of the fluid domain in tube, m^2
h_w	–	heat transfer coefficient (water side), $W/(m^2\ K)$
k	–	turbulence kinetic energy per unit mass, m^2/s^2
$\dot{m}_w$	–	mass flow rate of water, kg/s
q_w	–	wall heat flux, W/m^2
p_g	–	operating pressure (combustion gas side), bar
p_w	–	operating pressure (water side), bar
T_f	–	temperature of fluid in a control volume, K
T_{g-in}	–	temperature of the combustion gas at the inlet, K
T_{g-out}	–	temperature of the combustion gas at the outlet, K
T_w	–	temperature of wall, K
T_{w-in}	–	temperature of the water at the inlet, K
T_{w-out}	–	temperature of the water at the outlet, K
u^o	–	free stream velocity, m/s
$\bar{u}_c$	–	area averaged velocity (related to cross – sectional area of fluid domain in collector), m/s
$\bar{u}_{in}$	–	area averaged velocity (related to cross – sectional area of fluid domain at the inlet), m/s
$\bar{u}_t$	–	area averaged velocity (related to cross – sectional area of fluid domain in tube), m/s
u_τ	–	frictional velocity, m/s
u^*	–	velocity scale in the logarithmic region of boundary layer, m/s
$\dot{V}_g$	–	volumetric flow rate of the combustion gas, m^3/s

Greek symbols

η_w	–	absolute viscosity of water, $N\ s/m^2$
λ_w	–	thermal conductivity of water, $W/(m\ K)$
ρ_w	–	density of water, kg/m^3
τ_w	–	shear stress, N/m^2

Dimensionless numbers

$\mathrm{Nu}_w = \frac{h_w d_m}{\lambda_w}$	–	Nusselt number for water
$\mathrm{Pr}_w = \frac{c_{pw}\eta_w}{\lambda_w}$	–	Prandtl number for water
$\mathrm{Re}_w = \frac{u\rho_w d_m}{\eta}$	–	Reynolds number for water
T^+	–	dimensionless temperature
y^+	–	dimensionless distance from the wall in linear region of turbulent boundary layer
y^*	–	dimensionless distance from the wall in logarithmic region of turbulent boundary layer

1 Introduction

High-performance heat exchangers, with elliptical tubes, are widely used in many industries just to mention chemical, petrochemical, automotive and many others. The name of such types of heat exchangers is associated with

the consistency of its structure. The heat exchangers are characterized with the large heat – exchange area and high thermal – efficiency. Their working principle is to heat or cool gaseous or liquid mediums rapidly. Additionally, they can operate as evaporators, as well as condensers. The main advantage of using such energetic devices is the size of the heat exchange area as compared to a compact volume. For this reason, it is possible to use them as elements for easy installation in heating, drying, air-conditioning, technological and other systems.

The high efficiency of the type of heat exchangers is achievable thanks to the large packed fins on a tube surface. The dense packed rectangular fins increase the performance of a device significantly. To provide the stable heat transfer conditions, it is necessary to ensure the uniform or nearly uniform distribution of the velocity in all the tubes. Not fulfilling this condition may result in significant differences in the tube mean temperatures, then in occurrence of the excessive thermal stresses, and consequently lead to the heat exchanger breakedown. The working regime of this kind of heat exchangers implicates the possibility of the improper flow condition in tubes and collectors, causing unsuitable distributions of thermal and mechanical loads inside. The images of damaged tube, the Fig. 1 and 2, show that such a failure is possible.

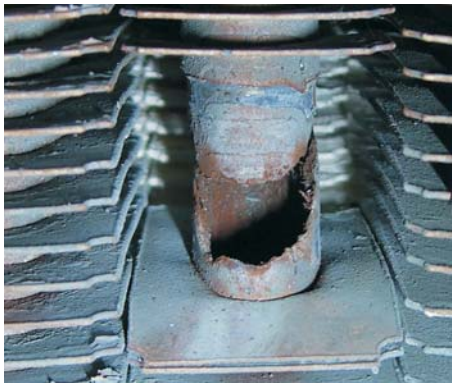

Figure 1. The fractured tube.

Figure 2. The buckled tube bundle.

It is possible to observe the existence of cavitations and erosion on the inner surface of the elliptical tube in the Fig. 1. The Fig. 2 shows the buckled

tube bundle. The excessive compressive stresses acting on the tubes result in the failure of the heat exchanger. It can be predicted, analyzing these figures, that unsuitable flow conditions in the heat exchanger caused the increase of the thermal stresses and damaged the tube consequently.

This paper presents the analysis of the flow condition in the high performance heat exchanger. The emphasis is put on the influence of the flow distribution on heat transfer. Furthermore, the possibility of cavitation occurrence is investigated. The nozzle spacing and dimensions of the heat exchanger are similar to the ones used in the industry. The widely used CFD [1–6] computations, necessary to explore the flow behavior, are carried out using the commercial code Ansys CFX.

2 Heat exchanger working conditions

The model of a two-pass high performance heat exchanger is presented schematically in Fig. 3.

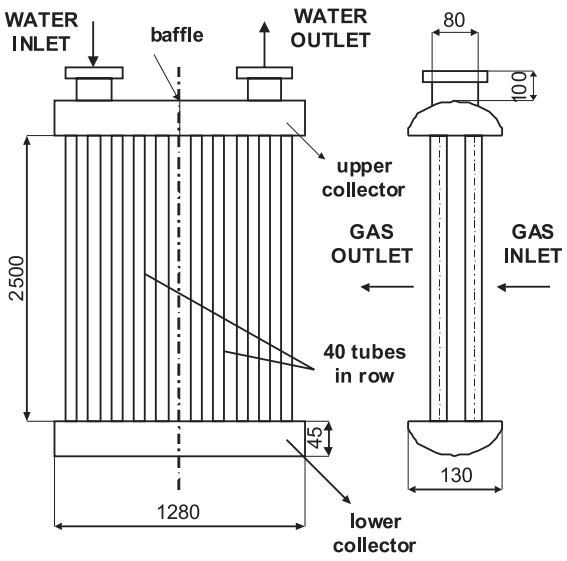

Figure 3. The scheme of a heat exchanger.

A single element of the main part of this heat exchanger – an elliptical tube with fins attached to it – is shown in Fig. 4. Besides to the large heat transfer area, this fin – tube assembly is characterized by the aero-dynamical shape,

low-pressure losses, and low sensitivity to pollution of the heat transfer area in the demanding working conditions. The zinc coating of the fins improves their corrosion resistance and extends their working lifetime.

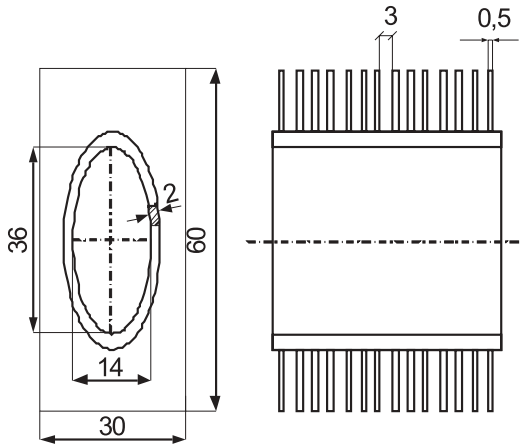

Figure 4. The elliptical tube – rectangular fin assembly.

The working regime of the investigated high-performance heat exchanger is given below. The combustion gas flows through the tubes bundle perpendicularly and is cooled by exchanging its heat with the water flowing inside the tubes. The working parameters of the heat exchanger that failed are presented in Tab. 1.

Table 1. Working parameters of the heat exchanger.

Flow parameter	Value
$\dot{m}_w$ [kg/s]	20
p_w [bar]	6
T_{w-in}/T_{w-out} [K]	383 / 403
$\dot{V}_g$ [m^3/s]	45
p_g [bar]	1.015
T_{g-in}/T_{g-out} [K]	723 / 663

The tracks of corrosion and erosion on the inner surface of the elliptical tube indicate the destructive impact of the flow on the tube. Moreover, the pieces of mounting boiler scale on the inner surface of the elliptical tube are

visible. The reason for this occurrence is the improper flow distribution in the device, that impairs the heat transfer conditions significantly. In this case, because of the lack of the liquid flow, the water does not absorb the heat properly. Consequently, the wall temperature increases dramatically, so does the effort of the material to balance the raising heat loads. The CFD computations are performed for flow parameters given in Tab. 1, to check in the regions of the heat exchanger where the danger of undesirable significant thermal loads exists.

3 Numerical modeling procedure

The critical zone consists of the three tubes presented on the Fig. 5. The rightmost tube is the one in which the failure occurred. The velocity, the heat transfer coefficient, the temperature and the pressure distribution along all the three critical tubes are investigated in this work.

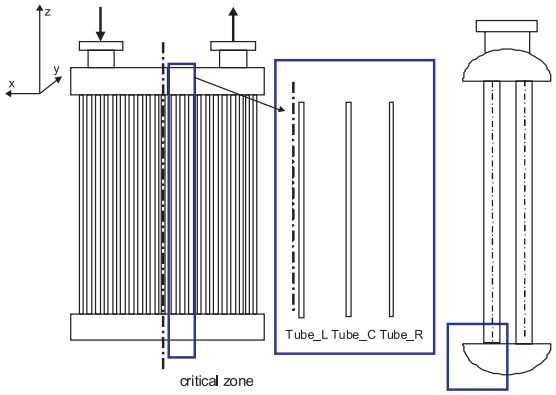

Figure 5. The variable position of the inlet nozzle pipe and three critical tubes.

As mentioned before, the impaired heat transfer conditions are the reason for the heat exchanger failure. Two phenomena associated with the impaired heat transfer in the device are cavitation and mounting of the boiler scale. Therefore, to settle the matter why the tube presented in Fig. 1 was damaged, it is essential to answer to the following questions:

- Are there conditions that favor the start-up and development of the cavitation process in the tube?
- Is it possible for the scale mounting process to begin?

To answer these questions it is necessary to know the heat transfer conditions, therefore the water – side heat transfer coefficient h_w and the temperature distribution along the tube are investigated. The next subsection explains how the h_w coefficient and the temperature in the control volume of the liquid domain are computed using CFX.

However to verify the computational procedure described below the test computation is carried through. It is the investigation of the flow in the part of the heat exchanger, rather than in the whole heat exchanger as in the exact simulations. The computations using k-ε and SST turbulence models are carried out. The limited flow domain (4 tubes and a part of upper collector) allows to increase the mesh resolution in the near wall region significantly, and resolve the boundary layer (5 elements are covering the boundary layer thickness $\delta = 1$ mm). In this case the SST [7] model, that is accurate in the near wall region, is used.

The results of h_w calculated for SST model are compared with the results obtained from the k-ε turbulence model. The numerical grid for k-ε turbulence model, used in the test simulations, is coarser than for the SST. The element length e_l equals 2 mm for the k-ε model and 1 mm for the SST. The boundary layer of the k-ε model is being modeled using only the wall functions as in the exact simulations.

The comparison of the results obtained using the k-ε and the SST turbulence models indicated the differences up to 10%. This accuracy is sufficient when indicating the zones and locations in the heat exchanger where the liquid distribution is improper.

3.1 Computation of the wall heat transfer coefficient

As aforementioned to state how the heat is distributed in and out of the flow domain it is necessary to calculate the temperature of water and its heat transfer coefficient h_w. To calculate the heat transfer coefficient h_w it is necessary to analyze the velocity boundary layer and similarly the thermal boundary layers. There are many analytical and experimentally combined approaches to investigate the flow behavior in a vicinity of the wall [8–10]. The velocity boundary layer is schematically presented in Fig. 6. The standard near – wall flow functions are used in this work for the k-ε turbulence model in Ansys CFX.

It is possible to compute h_w on the basis of the near wall functions, which estimates the near wall temperature T^+. The non dimensional temperature T^+ is a function of the dimensionless distance of the wall y^+ and

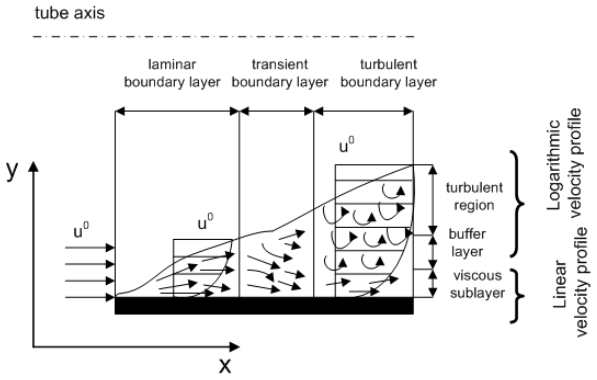

Figure 6. Boundary layer regions.

the Prandtl number Pr. The y^+ is defined as:

$$y^+ = \frac{\rho_w \Delta y \, u_\tau}{\eta_w} \, , \tag{1}$$

where Δy is the distance between two subsequent off wall grid nodes, η_w is the dynamic viscosity of water, and u_τ is the frictional velocity, which is the function of the shear stress τ_ω and the fluid density:

$$u_\tau = \left(\frac{\tau_\omega}{\rho} \right)^{\frac{1}{2}} \, . \tag{2}$$

According to Apsley [11] the near wall non dimensional temperature T^+ can be calculated:

- in the viscous sublayer using the linear formula:

$$T^+ = y^+ \mathrm{Pr}_w \, , \tag{3}$$

- in the buffer and turbulent layer using the logarithmic rule:

$$T^+ = \frac{\mathrm{Pr}_w}{\kappa} \ln y^+ + A(\mathrm{Pr}_w) \, , \tag{4}$$

  where $\kappa = \lambda_w / (c_{pw} \rho_w)$, and $A(\mathrm{Pr})$ can be estimated using the equation:

$$A(\mathrm{Pr}) = 13 \mathrm{Pr}_w^{\frac{2}{3}} - 7 \, . \tag{5}$$

The more sophisticated expression defining T^+ developed by Kader [12] is being used in the CFX computation. It is also basing on the log rule in the buffer and the turbulent regions of the boundary layer. In the log region, the Ansys developed the new velocity scale $u*$ to avoid singularity at separation points:

$$u^* = C_\mu^{\frac{1}{4}} k^{\frac{1}{2}} , \tag{6}$$

where the constant C_μ equals to 0.09 and k is a kinetic turbulence energy per unit mass, defined as:

$$k = \frac{1}{2}(\bar{u}_x^2 + \bar{u}_y^2 + \bar{u}_z^2) , \tag{7}$$

where $\bar{u}_x, \bar{u}_y, \bar{u}_z$ are the mean of velocity components fluctuation.

The non-dimensional distance from the wall for the log-rule region is defined as:

$$y^* = \frac{\rho_w u^* \Delta y}{\eta_w} . \tag{8}$$

Finally, the Kader's formula that allows computing T^+ is:

$$T^+ = \mathrm{Pr}_w y^* e^{-\Gamma} + (2.12 \ln(y^*) + \beta) e^{(\frac{-1}{\Gamma})} , \tag{9}$$

where the variable $\Gamma = f(\mathrm{Pr}_w, y^*)$ and $\beta = f(\mathrm{Pr}_w)$.

The wall heat flux q_w is determined from the equation:

$$q_w = \frac{\rho_w c_{pw}\, u^*}{T^+}(T_w - T_f) = h_w(T_w - T_f) . \tag{10}$$

The c_{pw} is the specific heat capacity of fluid, and T_w and T_f are the temperatures of the wall and of the fluid node nearest to the wall.

The wall heat flux q_w that allows to obtain the mass flow average outlet temperature of the water $T_{w-out} = 403$ K may be computed from the series of CFD simulations, starting from the low guess value and then gradually increased until the desirable T_{w-out} is reached. Subsequently this heat flux is stated as a boundary condition for the proper simulation. For the presented computational case q_w equals to 150000 W/m^2. The q_w is multiplied by the surface area and added to the boundary energy control volume equation. From the energy balance of the control volume the code computes T_f. The water parameters like ρ_w, η_w and c_{pw} are calculated for its value. Next, the momentum equation, including the turbulence model, is solved and the k value is computed to obtain the values of u^* and y^*. Finally T^+ is obtained.

After this computation loop the heat transfer coefficient h_w is calculated from the equation:

$$h_w = \frac{\rho_w c_{pw} u^*}{T^+} \,. \tag{11}$$

3.2 Velocity scales and turbulence model

The general information about the flow regime is obtained from the calculations on the basis of the data from Tab. 1.

The mean velocity at the inlet domain is calculated according to the formula:

$$\bar{u}_{i_n} = \frac{\dot{m}_w}{\rho_w F_{in}} \,. \tag{12}$$

The mean velocity in a tube domain in the first pass is calculated from the equation:

$$\bar{u}_t = \frac{\dot{m}_w}{\frac{n}{2}\rho_w F_t} \,, \tag{13}$$

where n is the number of pipes in the whole heat exchanger.

The mean velocity in a lower collector domain can be obtained from the equation:

$$\bar{u}_c = \frac{\dot{m}_w}{\rho_w F_c} \,. \tag{14}$$

In Tab. 2 the calculated Reynolds numbers are presented. The calculations show that the flow regime is turbulent. The used k-ε turbulence model, widely discussed in the literature [13–16], is the robust option for the complex flow geometry used.

Table 2. The Reynolds number values for different flow domains.

Location	F[m^2]	$\bar{u}$ [m/s]	Re$_w$ [–]
Inlet	$3.7{\cdot}10^{-3}$	5.7	$1{\cdot}10^{6}$
Tube	$4.1{\cdot}10^{-4}$	1.26	$9.3{\cdot}10^{4}$
Collector	$5{\cdot}10^{-3}$	4.14	$1.23{\cdot}10^{6}$

This model uses the standard near-wall functions. Because these functions are the approximation of the liquid behavior in the near-wall region, it is necessary to validate the results using the experimental data. Therefore,

the determined heat transfer coefficients h_w, are compared with the well known Dittus-Boelter correlation [17]:

$$\mathrm{Nu}_w = 0.023\mathrm{Re}_w^{0.8}\mathrm{Pr}_w^{0.4} \,. \tag{15}$$

The comparison between the Dittus-Boelter correlation and the thermal boundary layer theory is presented in the next section.

4 Results and discussion

In this section the results of the CFD computation are shown and discussed. At first, the streamlines that show the flow distribution are presented for the entire heat exchanger. Next, the closer focus is made on the flow in the upper and the lower collectors.

Diagrams of heat transfer coefficient h_w and area averaged velocity along the tube length distribution for three critical tubes (see Fig. 5) are presented. The area-averaged velocity is necessary for the calculation of h_w according to the Dittus-Boelter correlation, see Eq. (15).

In order to check the stability of solution, the computations are carried out for three different numerical grid densities. The element edge length e_l equals to 3 mm, 2 mm and 1 mm for subsequent computations. The difference between the computed results for $e_l = 1$ mm and 3 mm in the critical zones are up to 5%. The results obtained from the computations when e_l is equal to 1 mm and 2 mm differ by up to 2 % in the critical zones. Regardless to the hardware resources, the $e_l = 2$ mm is sufficient to obtain accurate results in a reasonable time. The results for $e_l = 2$ mm are presented in the next subsections.

The convergence is reached, during the computational process, when the RMS normalized residuals are less than 0.0001 for the momentum, continuity and turbulence model equations.

Finally, the temperature distribution and the pressure value is presented for critical tubes. According to these results, the discussion on the possibility of the cavitation and the mounting of boiler scale occurrence is carried out.

4.1 Analysis of flow distribution

The streamlines are presented in Fig. 7. It is possible to observe, that there are strong differences in values of velocity in the tubes. Moreover, the lack

of streamlines in many tubes (the white areas) indicates, that the water doesn't flow, or flows with very low speed in these tubes. This improper flow distribution and the tube feeding may cause large increase in the fluid temperature, which may exceed the boiling point temperature of water for the local value of pressure. The undesirable consequence of it is the rapid phase change and cavitation.

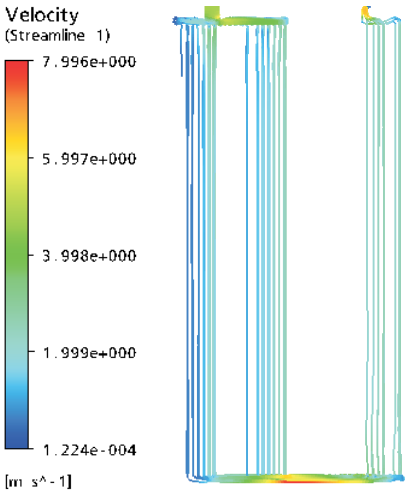

Figure 7. Distribution of streamlines.

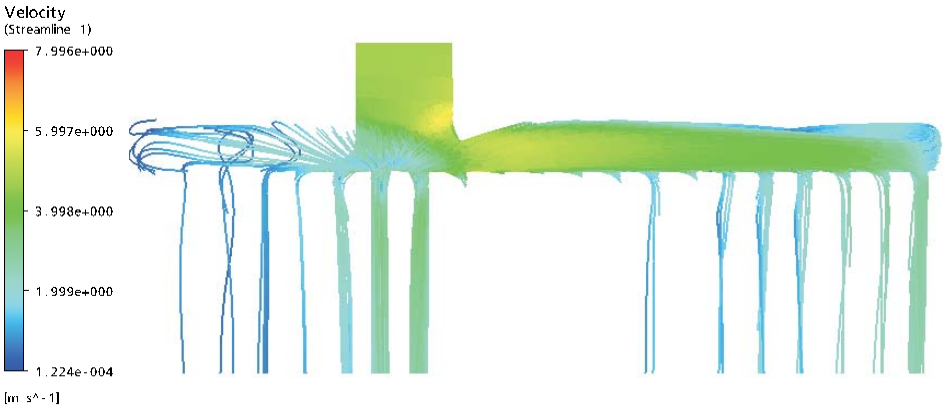

Figure 8. The streamlines in the upper collector of heat exchanger.

The Fig. 8 shows how water flows from the upper collector to tubes. The water is supplied properly only to the tubes which are the nearest to supply pipe. Because of the horizontal direction of the main stream, only a few of the tubes near the axis of the heat exchanger and the leftmost ones are fed with the sufficient amount of liquid. There is a danger that the first pass of water doesn't flow or flows with very low speed in the majority of tubes, causing the liquid temperature to increase significantly. Such rapid increase in temperature is the reason for the undesirable significant thermal loads along the tube. Therefore, the tubes are subjected to strong compressive forces, which may cause the buckling.

The distribution of streamlines in the vicinity of the lower collector is shown in Fig. 9. The main conclusion may be drawn, basing on the image, is that the most of the tubes from the second pass are not fed properly.

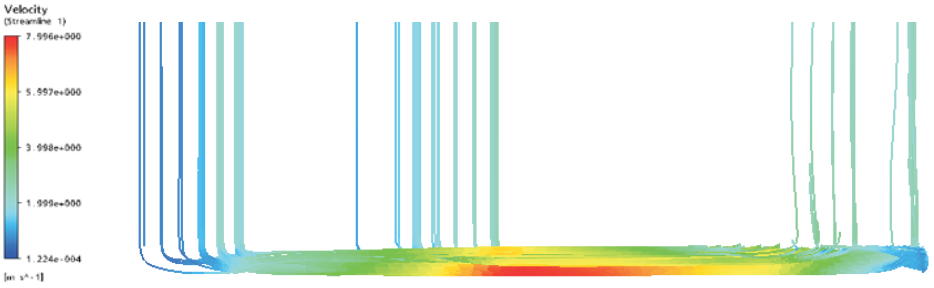

Figure 9. The streamlines in the lower collector of the heat exchanger.

The main stream flows in the horizontal direction with the speed exceeding 7 m/s. Consequently, when the liquid tries to change its direction and to enter the tubes, the recirculation zones and vortices (see the Fig. 10) occur. Their occurrence is dangerous because of the local pressure drop, that facilitates the cavitations process, when the temperature exceeds the boiling point of water. The destroying impact of cavitations on the tube material is the reason, why the inner surface of the damaged tube presented in Fig. 1 is eroded.

4.2 Heat transfer in critical tubes

The distribution along the tube length of the area averaged velocity v_a for three critical tubes is shown in Fig. 11. The values of v_a are the highest in tube L. However, it is still low in comparison to the tubes that are

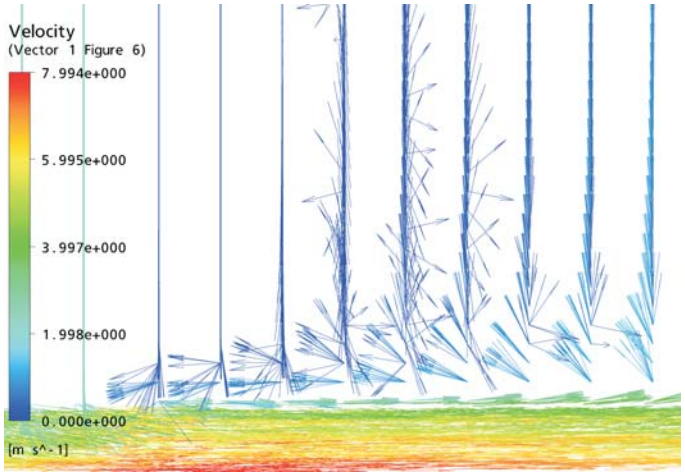

Figure 10. The recirculation zones in the lower collector.

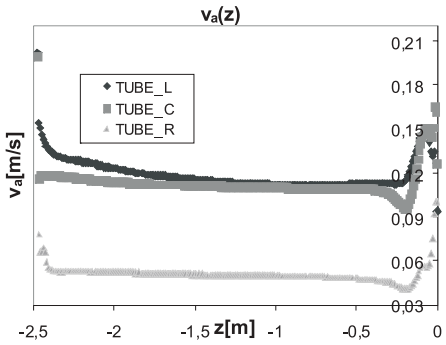

Figure 11. The area averaged velocity in three critical tubes.

fed properly with water, and where the value of v_a exceeds 2 m/s. This means, that the heat transfer coefficient in all the three tubes, calculated according to the boundary layer theory (Fig. 12), has relatively low values and temperature there can exceed the temperature of the boiling point of water for the local pressure.

The values of h_w computed according to the Dittus–Boelter correlation are shown in Fig. 13. The calculated values of the heat transfer coefficient are lower than the ones obtained from the boundary layer theory. It is so, because the different calculation procedure is used. The heat transfer coefficient is averaged for the Dittus–Boelter correlation, with respect to

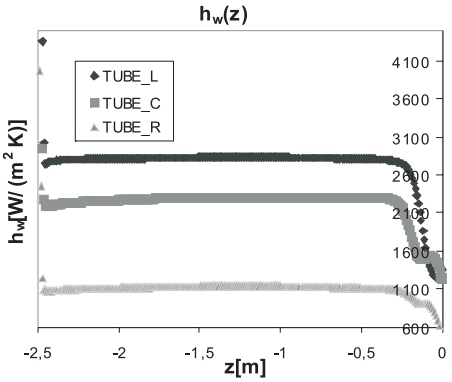

Figure 12. The heat transfer coefficient along three critical tubes – thermal boundary layer theory.

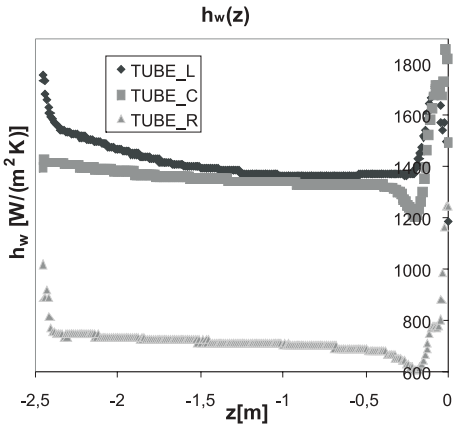

Figure 13. The heat transfer coefficient along three critical tubes, according to Dittus-Boelter.

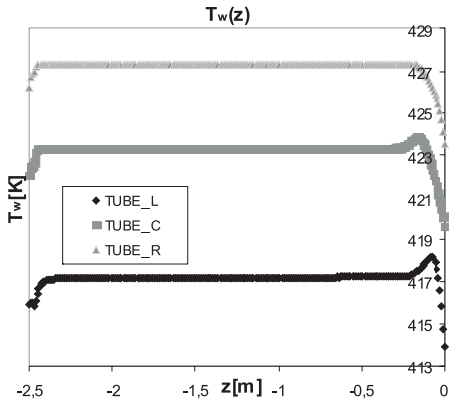

Figure 14. The temperature distribution along three critical tubes.

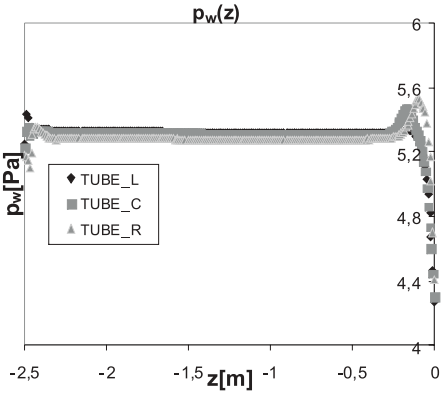

Figure 15. The pressure distribution along three critical tubes.

the mean velocity and to the mean temperature at the inlet. In case of the boundary layer theory, the heat transfer coefficient is calculated with respect to the local temperature of liquid in the control volume T_f and to the local value of the velocity in control volume.

The temperature distribution along three critical tubes is shown in Fig. 14. The boiling point of water temperature for $p_w = 6$ bar equals to 431 K. The temperature in the rightmost tube is slightly below this value. However, as aforementioned, the recirculation zone (see Fig. 10), may cause the operating pressure to drop. It is possible to observe in Fig. 15, that the local value of pressure in the critical tubes is lower than 6 bars. The boiling point temperature equals 425 K for the operating pressure of 5.1 bar, and is exceeded in the rightmost tube. Therefore, the cavitation is probable to occur there.

Furthermore, when the liquid flows through the tubes with a very low speed and its temperature exceeds the temperature of the boiling point, the facilitating conditions exist for starting the mounting process of the boiler scale. This happened in the rightmost tube – "Tube_R" and accelerated the failure process.

5 Conclusions and outlook

The present work demonstrates the flow field in the main parts of high-performance heat exchanger. The CFD computations indicate that the occurrence of vortices zones is possible that drastically decrease the pressure value, due to the fully developed turbulent flow regime and complicated geometry of flow domains. As a result, the cavitation process occurs, deteriorating the local heat transfer conditions significantly. Therefore, the large increase in the wall temperature happens, bringing about the additional considerable thermal loads that act on the tubes.

Now the thermo-mechanical analysis are carried out to investigate the influence of the heat transfer conditions on the stress field in the heat exchanger. It can be concluded upon the load cases, that the strong vortices zones form inside collectors and tubes. The results of these computations will be presented in the future.

Received 15 June 2010

References

[1] Hoffman K.A., Chiang S.: *Computational Fluid Dynamics*, Vol. 1–3. EES, 2000.

[2] Chung T.J.: *Computational Fluid Dynamics*. Cambridge Univ. Press., Cambridge 2002.

[3] Wesseling P.: *Principles of Computational Fluid Dynamics*. Springer, Heideberg 2000.

[4] Srnivas K., Fletcher C.A.J.: *Computational Techniques for Fluid Dynamics*. Springer, New York 1992.

[5] Tannehill J.C., Anderson D.A., Pletcher R.H.: *Computational Fluid Mechanics and Heat Transfer*. Taylor and Francis, Washington 1997.

[6] Ferziger J.H., Perič M.: *Computational Methods for Fluid Dynamics*, Springer, 2002.

[7] Menter F.R.: *Zonal two equation k-ω turbulence models for aerodynamic flows*. AIAA Paper 93-2906, 1993.

[8] White F.M.: *Fluid Mechanics*. McGraw, New York 2006.

[9] Incopera F.P., Dewitt D.P.: *Introduction to Heat Transfer*, 2nd edn. Wiley, 1990.

[10] Incopera F.P., Dewitt D.P., Bergman T., Lavine A.: *Fundamentals of heat and mass transfer*. Willey, Los Angeles 2007.

[11] Apsley D.: *Boundary Layer Spring School 2009*. University of Manchester, 2009.

[12] Kader B.A.: *Temperature and concentration profiles in fully turbulent boundary layers*. Int. Journal of Heat and Mass Transfer **24**(1981), 9, 1541–1544.

[13] Date A.W.: *Introduction to Computational Fluid Dynamics*. Cambridge University Press, New York 2005.

[14] Wilcox D.C.: *Turbulence Modeling for CFD*. DCW Industries, Glendale 1993.

[15] Blazek J.: *Computational Fluid Dynamics Principles and Applications*. Elsevier, Oxford 2001.

[16] Cebeci T., Shao J.P., Kafyeke F., Laurendau E.: *Computational Fluid Dynamics for Engineers*, Springer, Long Beach 2005.

[17] *Heat Exchanger Design Handbook*. VDI, Düsseldorf 1983.